Low-loss and low-bend-sensitivity mid-infrared guidance in a hollow-core–photonic-bandgap fiber

Natalie V. Wheeler,* Alexander M. Heidt, Naveen K. Baddela, Eric Numkam Fokoua, John R. Hayes, Seyed R. Sandoghchi, Francesco Poletti, Marco N. Petrovich, and David J. Richardson

Optoelectronics Research Centre, University of Southampton, Southampton SO17 1BJ, UK
**Corresponding author: n.v.wheeler@soton.ac.uk*

Received October 10, 2013; revised November 21, 2013; accepted November 22, 2013;
posted December 4, 2013 (Doc. ID 199294); published January 8, 2014

Hollow-core–photonic-bandgap fiber, fabricated from high-purity synthetic silica, with a wide operating bandwidth between 3.1 and 3.7 μm, is reported. A minimum attenuation of 0.13 dB/m is achieved through a 19-cell core design with a thin core wall surround. The loss is reduced further to 0.05 dB/m following a purging process to remove hydrogen chloride gas from the fiber—representing more than an order of magnitude loss reduction as compared to previously reported bandgap-guiding fibers operating in the mid-infrared. The fiber also offers a low bend sensitivity of <0.25 dB per 5 cm diameter turn over a 300 nm bandwidth. Simulations are in good agreement with the achieved losses and indicate that a further loss reduction of more than a factor of 2 should be possible by enlarging the core using a 37-cell design. © 2014 Optical Society of America

OCIS codes: (060.5295) Photonic crystal fibers; (060.2280) Fiber design and fabrication.
http://dx.doi.org/10.1364/OL.39.000295

Conventional all-solid optical fibers have revolutionized many fields, starting with telecommunications and branching to areas as diverse as fiber optic gyroscopes and other sensors, high-power fiber lasers, and endoscopes for medical applications [1,2]. The spectral range where conventional fibers have made the greatest impact has been largely defined by the transparency window of silica glass, which is usually the main constituent of these fibers. High-purity, dry synthetic silica (e.g., Suprasil F300 from Heraeus) is transparent (<10 dB/km [3]) between ~500 and 2000 nm, and limited at short wavelengths by electronic absorption and at longer wavelengths by multiphonon absorption. The fabrication of low-loss, durable, and bend-insensitive fibers at wavelengths extending to longer wavelengths and into the mid-infrared (mid-IR) is desirable for applications including high-power laser beam delivery, gas sensing, gas lasers, and surgery.

Toward this goal, several avenues have been explored, starting with chalcogenide glasses and followed by fluoride, polycrystalline, and tellurite fibers (see [4] for a review). While low attenuation values have been achieved (e.g., 0.45 dB/km in a ZBLAN fiber [5]), a mid-IR fiber has not yet been able to provide the combination of durability, bend insensitivity, modal quality, and power handling offered by silica-based fibers in the near-IR. Hollow-core fibers offer an attractive alternative [6], where the majority of light is guided in air, or a controlled composition of gas, minimizing loss contributions from material absorption. Guidance in a hollow core also offers a higher damage threshold and additional functionalities leading to further applications such as gas sensing and quantum optics [7,8]. This is particularly of interest in the mid- to far-IR where the fundamental vibrational lines of molecular species lie; these resonances are inherently stronger than those in the near-IR, indicating the potential for high-precision spectroscopy at ultralow pressures and gas sensors with faster response times. Hollow-core silica-based fibers have recently been reported that deliver optical guidance up to 7.9 μm [9], sparking a revival of interest in this fiber composition for mid-IR applications. In particular, Yu *et al.* [10] reported a loss of 34 dB/km at 3.050 μm in combination with a broadband low-loss guidance region extending from 2.85 to 3.85 μm. This loss figure is truly remarkable considering the attenuation of bulk dry synthetic silica ranges from 60 up to more than 600 dB/m in this spectral region [3]. These recently reported fibers confine light in the fiber core through antiresonance (AR) within the core surround, enhanced by a negative curvature core design [11], and low loss is in part achieved through a large core diameter (e.g., 94 μm [10]), which minimizes overlap between the core modes and the silica regions of the fiber. This large diameter, while suited for some applications, can restrict the use of these fibers due to the challenge of achieving low-loss coupling to conventional step index IR fibers. Furthermore, due to the leaky guidance mechanism, AR fibers are extremely bend sensitive, preventing a compact device footprint and/or limiting the maximum usable operating lengths.

Hollow-core–photonic-bandgap fibers (HC-PBGFs) provide an alternative mechanism for light confinement in an air-core fiber. Until now, the lowest reported loss in this spectral region was ~1 dB/m [12] in a seven-cell fiber operating at wavelengths up to 3.4 μm. Here we report a 19-cell HC-PBGF that demonstrates an order of magnitude reduction in loss (0.13 dB/m at 3.33 μm) in combination with a wide operating bandwidth, extending from 3.1 to 3.7 μm, and that also exhibits very low bend sensitivity. Furthermore, we show, for the first time, to the best of our knowledge, experimental results confirming that unwanted absorption features due to HCl in the hollow core can be successfully removed through gas purging. Transmission loss measurements in the near-IR show that in addition to the fundamental bandgap guidance in the mid-IR, several further low-loss spectral regions exist with losses as low as 1.2 dB/m. The origin of this guidance is discussed. Finally, we present simulations of the fiber characteristics based on the structure of the fabricated fiber that are in good agreement with the achieved minimum loss.

The HC-PBGF has a 19-cell core design and was fabricated using the conventional two-step stack and draw

technique. The differential pressure between the core and cladding regions of the structure was carefully controlled during the fiber drawing process to maintain an optimum core surround and to minimize the overlap between the core guided modes and the silica core surround. This approach, combined with a thin-walled core surround, is necessary to enable a wide, surface mode free operating bandwidth [13]. A scanning electron microscope (SEM) image of the fabricated fiber is shown in Fig. 1(a); the average core diameter is 50 μm, the average hole-to-hole distance is 9.3 μm, and the relative hole size [14] is 0.965.

The fiber transmission in the mid-IR [Fig. 1(b)] was recorded using a custom built supercontinuum source that generates a broad spectrum spanning from 0.75 to 4 μm by pumping a ZBLAN fiber with a diode-seeded picosecond thulium-doped fiber amplifier system at 2 μm [15]. A monochromator with ~5 nm resolution was used for detection of the signal transmitted through the PBGF. The measurement over a 5 m fiber length [purple line in Fig. 1(b)] shows that the bandgap extends from 3.1 to 3.8 μm and a cutback loss measurement (58 to 5 m) shows a minimum loss of 0.13(±0.05) dB/m at 3.33 μm and <1 dB/m transmission loss over >500 nm bandwidth despite the high bulk silica attenuation. The uncertainty associated with this measurement arises from a combination of source instability [15] and variations in the fiber cleave. This low-loss value indicates that the average overlap between the core guided modes and the silica surround is less than 0.3%.

At the short wavelength edge of the bandgap, there are several loss peaks that we believe are due to surface modes, while between 3.3 and 3.6 μm many gas absorption lines are visible. These can be attributed to HCl absorption; this gas is present in the fiber due to the use of chlorine to dehydrate the bulk silica glass that is used as the raw material in fabrication [16]. Figure 2(a) shows the theoretical HCl absorption lines in this spectral region [17]; the excellent agreement between this data and the observed loss peaks in experimental loss measurement confirms that their origin is HCl absorption. The measured minimum loss lies

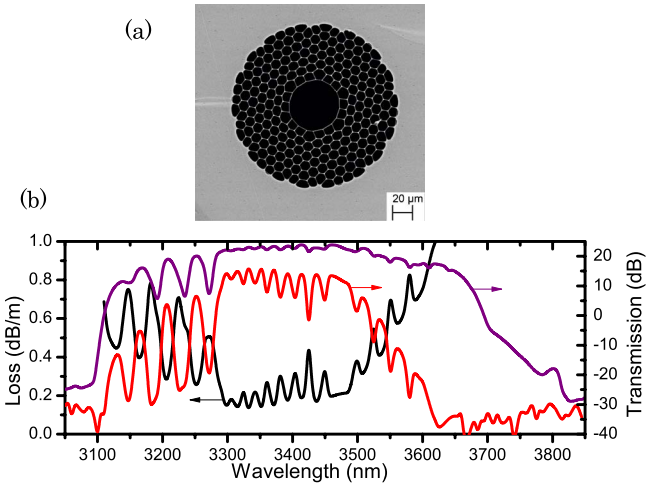

Fig. 1. (a) SEM of fabricated fiber. (b) Transmission through 5 m (purple line) and 58 m (red line) and corresponding attenuation calculated from cutback measurement (black line).

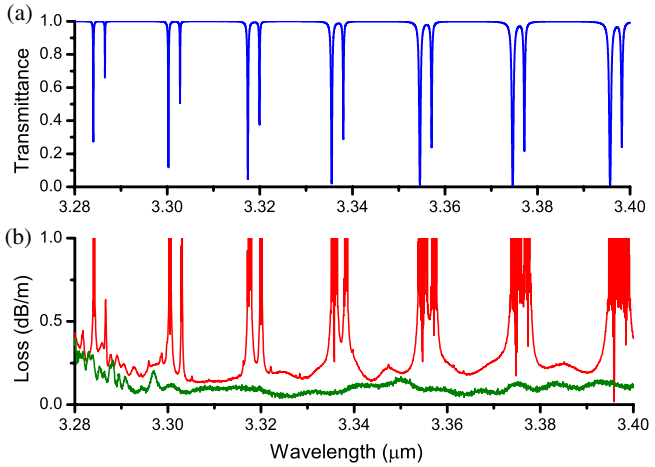

Fig. 2. (a) HCl absorption spectrum taken from HITRAN database. (b) High-resolution attenuation measurements (0.2 nm) measured by cutback technique before and after purging the HC-PBGF with argon for five days (red and green lines, respectively). Cutback lengths were from 53 to 5 m and 48 to 5 m, respectively.

between two such absorption lines, and it is likely that the loss value would be lower if the gas was eliminated from the fiber. Note that the loss measurement shown in Fig. 1(b) is limited by the 5 nm resolution of the monochromator. Furthermore, due to the large mismatch between the launch ZBLAN fiber (9 μm core diameter) and the HC-PBGF, excitation of higher-order modes in the latter is almost inevitable, which will most likely lead to a loss overestimate.

In order to investigate the dynamics of the HCl gas and the possible limitations that the presence of this gas may place on the use of HC-PBGF in this spectral region, we purged 53 m of the fiber for five days. The input end was attached to a reservoir of 6 bar, high-purity argon gas, while the output end was left open to atmosphere. Figure 2(b) shows cutback loss measurements for the fiber before and after purging. These measurements were recorded using a Yokogawa optical spectrum analyzer that operates at wavelengths up to 3.4 μm and enables high-resolution data (0.2 nm presented here) to be recorded. It is clear from Fig. 2 that purging for a reasonably short time completely removes the HCl gas from the fiber. Furthermore, the measured minimum fiber loss after purging was reduced to 0.05 ± 0.03 dB/m. The oscillations remaining in the loss spectrum are believed to originate from modal interference.

The bend loss of the HC-PBGF was measured by comparing the transmission through a 5 m length, which included five coils of 5 cm diameter, with the same fiber only loosely coiled. These spectra, along with the resultant bend loss per turn, are shown in Fig. 3. This measurement shows the bend loss is <0.5 dB/turn over the entire surface mode free region of the bandgap and <0.25 dB/turn over a 300 nm bandwidth. This loss is significantly lower than that reported recently for AR fibers operating in the same wavelength region (e.g., ~6 dB loss for a ~20 cm diameter coil [10]) and indicates that this fiber is well-suited for the fabrication of compact gas cells for sensing and spectroscopy. It is also important

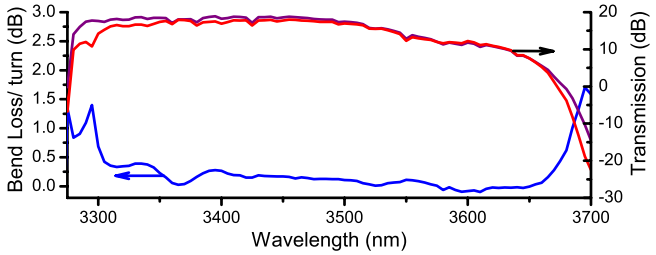

Fig. 3. Bend loss: transmission of 5 m of the HC-PBGF was recorded with five coils of 5 cm diameter in the fiber (red line) and with the fiber loosely coiled (purple line). The bend loss per turn (blue line) is <0.25 dB over a 300 nm bandwidth.

to note that this measured bend loss could be due to bend sensitivity of the higher-order modal content of the fiber, as with conventional multimode step index fibers, and therefore the loss of the fundamental mode may well be lower and we can consider the measured value as an upper limit.

Several low-loss guidance windows were also observed in the visible and near-IR, with a minimum transmission loss of 1.2 dB/m at 1690 nm and several similar low-loss regions between 800 and 1000 nm, as shown by the cutback measurement in Fig. 4. This opens up the possibility of simultaneous guidance of both near and mid-IR light in this fiber. The presence of resonant loss features within this band is indicative of AR guidance, although it is possible that these low-loss regions could be attributed to narrow, higher-order bandgaps. AR guidance bands have been previously observed in the visible region in HC-PBGFs designed to operate at 1550 nm [18], with losses of the order of dB/cm, two orders of magnitude higher than the losses reported here. However, for a fair comparison it is important to note that those results were recorded at wavelengths around 600 nm in a fiber with a smaller core diameter (11.4 μm), so scattering due to surface roughness would have a much larger impact on attenuation than in the fiber reported here. From

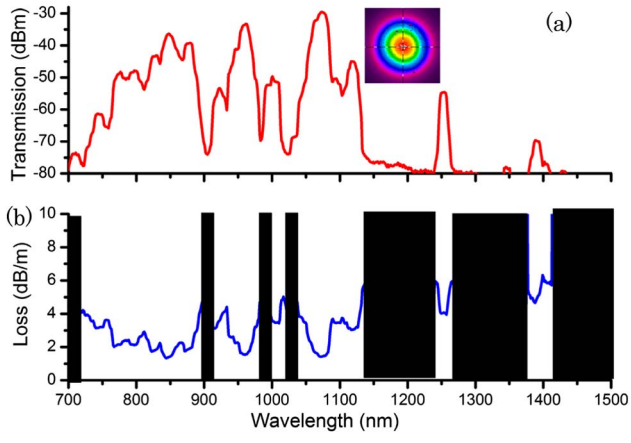

Fig. 4. (a) Transmission through 10 m of HC-PBGF recorded using a commercial supercontinuum source; the mode image shown in the inset was recorded at ~1.1 μm. (b) Attenuation of the HC-PBGF in the near-IR calculated by cutback to 5 m length. Blacked out regions correspond to effectively zero transmission.

the SEM image shown in Fig. 1(a), the core surround thickness was estimated as 180 ± 30 nm. From these measurements, resonance with the core surround would be expected at ~370 nm, with a broad AR region at longer wavelengths.

To gain further insight into this guidance mechanism, the bend loss in this spectral region was also recorded. In the low-loss regions of the near-IR guidance, the bend loss was ~0.8 dB per 8 cm diameter turn. For a fundamental bandgap operating in this spectral region, the bend losses are expected to be negligible [19], so this could support an AR guidance mechanism; however, the transmission properties of higher-order bandgaps in HC-PBGFs have not been extensively examined and studies in all-solid PBGFs have revealed complex bend sensitivity that does indeed increase with bandgap number [20]. Further work is underway to confirm the nature of the guidance mechanism that is appropriate here.

In order to assess the potential of improving this fiber design for lower loss operation in the mid-IR we first simulated the fabricated fiber to determine the agreement between the minimum attenuation achieved in the fabricated fiber and that expected theoretically. Fiber parameters, such as average cladding strut thickness and hole separation, were extracted from the SEM shown in Fig. 1(a) and used in a model based on the finite element method. The wavelength dependence of the attenuation of Suprasil F300 in this spectral range was extracted from [3]. The simulated fiber transmission is shown in Fig. 5(a); the minimum attenuation was found to be 0.07 dB/m for a core mode overlap with the silica structure of 0.1%. This is in good agreement, to within the associated uncertainty of the experimental minimum loss post purging. In contrast to HC-PBGFs operating in the near-IR, the loss is limited by the silica absorption instead of scattering due to surface roughness [21]. The dominance of silica absorption in defining the fiber attenuation is highlighted in Fig. 5(b), where confinement loss

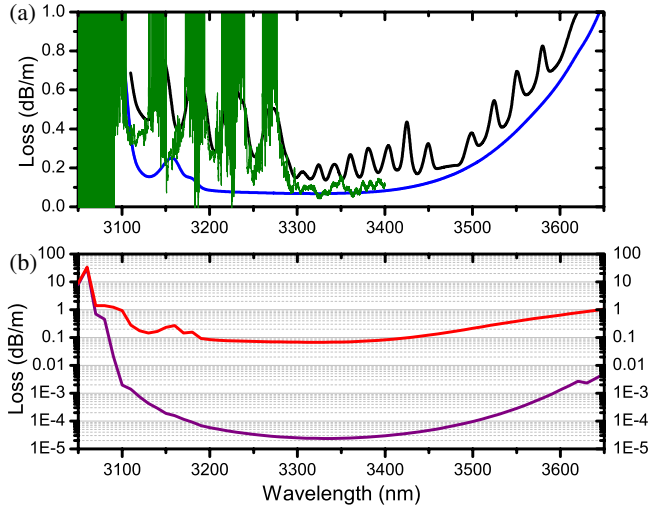

Fig. 5. (a) Simulated attenuation (blue line) is in good agreement with measured attenuation before and after purging (black and green lines with 5 and 0.2 nm resolution, respectively). (b) Breakdown of loss contribution; simulated confinement loss (purple line) is compared to total simulated loss (red line).

is plotted and compared with the total attenuation. From this figure it is clear that confinement loss is negligible compared to silica absorption for the fiber design operating in the mid-IR. Furthermore, two surface modes are indicated in the simulation, toward the short wavelength edge of the bandgap; the presence of these indicates that the loss peaks observed in this region of the bandgap in the experimental transmission are also due to surface modes.

To achieve lower losses using a bandgap fiber design, it will be necessary to reduce the overlap with the silica fiber cladding. The use of a 37-cell defect core to increase the core radius, which has already been demonstrated for data transmission applications [22], is expected to reduce the overlap by an additional 60%, indicating that losses can be reduced to achieve a level comparable with or in fact lower than state-of-the-art AR fibers operating in this spectral region [9,10], without compromising on bend sensitivity.

In conclusion, we have fabricated and characterized a 19-cell HC-PBGF that provides low-loss (<1 dB/m) guidance between 3.1 and 3.6 μm. The fiber has a record minimum attenuation of 0.13 dB/m at 3.33 μm for a HC-PBGF operating in the mid-IR, which reduced to 0.05 dB/m after purging to remove HCl gas. This low-loss operation is combined with an extremely low bend loss for this spectral region of <0.25 dB per 5 cm diameter turn over a 300 nm bandwidth making this fiber suitable for applications such as gas sensing and surgery, which may require a device with a small footprint and/or high flexibility. In particular, it is expected that a fiber with the same design but scaled to operate at 2.94 μm would be highly suited for Er:YAG laser delivery for high-precision medical applications, such as cutting through hard biological tissue [12]. Interestingly, low-loss guidance (1.2 dB/m) in the near-IR was also recorded in this fiber, the nature of which is yet to be confirmed, but an initial investigation indicates the possibility of antiresonant guidance. Due to this near-IR transmission, this fiber may be a suitable host for a hollow optical fiber gas laser that is pumped in the near-IR and lases in the mid-IR [23]. By enlarging the core to a 37-cell defect, in order to reduce the overlap of the core guided mode with the silica cladding, it is anticipated that losses can be reduced further without increasing the bend sensitivity.

This work was supported by the UK EPSRC through grants EP/I01196X/1 (HYPERHIGHWAY) and EP/H02607X/1. A. M. H. acknowledges funding from the EU 7th Framework Program (Marie Curie Actions) under grant agreement 300859 (ADMIRATION). F. P. gratefully acknowledges support from the Royal Society.

References

1. B. Culshaw and A. Kersey, J. Lightwave Technol. **26**, 1064 (2008).
2. D. J. Richardson, J. Nilsson, and W. A. Clarkson, J. Opt. Soc. Am. B **27**, B63 (2010).
3. O. Humbach, H. Fabian, U. Grzesik, U. Haken, and W. Heitmann, J. Non-Cryst. Solids **203**, 19 (1996).
4. J. A. Harrington, *Infrared Fibers and Their Applications* (SPIE, 2004).
5. P. W. Carter, S. F. Moore, M. W. Szebesta, D. Williams, J. R. Ranson, and D. France, Electron. Lett. **26**, 2115 (1990).
6. J. M. Kriesel, N. Gat, B. E. Bernacki, R. L. Erikson, B. D. Cannon, T. L. Myers, C. M. Bledt, and J. A. Harrington, Proc SPIE **8018**, 80180V (2011).
7. F. Benabid, P. J. Roberts, F. Couny, and P. S. Light, J. Eur. Opt. Soc. Rapid Publ. **4**, 09004 (2009).
8. T. Ritari, J. Tuominen, H. Ludvigsen, J. H. Petersen, T. Sorensen, T. Hansen, and H. Simonsen, Opt. Express **12**, 4080 (2004).
9. A. N. Kolyadin, A. F. Kosolapov, A. D. Pryamikov, A. S. Biriukov, V. G. Plotnichenko, and E. M. Dianov, Opt. Express **21**, 9514 (2013).
10. F. Yu, W. J. Wadsworth, and J. C. Knight, Opt. Express **20**, 11153 (2012).
11. Y. Y. Wang, N. V. Wheeler, F. Couny, P. J. Roberts, and F. Benabid, Opt. Lett. **36**, 669 (2011).
12. A. Urich, R. R. J. Maier, B. J. Mangan, S. Renshaw, J. C. Knight, D. P. Hand, and J. D. Shephard, Opt. Express **20**, 6677 (2012).
13. F. Poletti, N. V. Wheeler, M. N. Petrovich, N. Baddela, E. N. Fokoua, J. R. Hayes, D. R. Gray, and D. J. Richardson, Nat. Photonics **7**, 279 (2013).
14. N. A. Mortensen and M. D. Nielsen, Opt. Lett. **29** 349, (2004).
15. A. M. Heidt, J. H. V. Price, C. Baskiotis, J. S. Feehan, Z. Li, S. U. Alam, and D. J. Richardson, Opt. Express **21**, 24281 (2013).
16. J. K. Lyngso, B. J. Mangan, C. Jakobsen, and P. J. Roberts, Opt. Express **17**, 23468 (2009).
17. L. S. Rothman, I. E. Gordon, A. Barbe, D. C. Benner, P. E. Bernath, M. Birk, V. Boudon, L. R. Brown, A. Campargue, J. P. Champion, K. Chance, L. H. Coudert, V. Dana, V. M. Devi, S. Fally, J. M. Flaud, R. R. Gamache, A. Goldman, D. Jacquemart, I. Kleiner, N. Lacome, W. J. Lafferty, J. Y. Mandin, S. T. Massie, S. N. Mikhailenko, C. E. Miller, N. Moazzen-Ahmadi, O. V. Naumenko, A. V. Nikitin, J. Orphal, V. I. Perevalov, A. Perrin, A. Predoi-Cross, C. P. Rinsland, M. Rotger, M. Simeckova, M. A. H. Smith, K. Sung, S. A. Tashkun, J. Tennyson, R. A. Toth, A. C. Vandaele, and J. Vander Auwera, J. Quantum Spectrosc. Radiat. Transfer **110**, 533 (2009).
18. R. E. P. de Oliveira, C. J. S. de Matos, G. E. Nunes, and I. H. Bechtold, J. Opt. Soc. Am. B **29**, 977 (2012).
19. T. P. Hansen, J. B. J. Broeng, C. Jakobsen, G. Vienne, H. R. Simonsen, M. D. Nielsen, P. M. W. Skovgaard, J. R. Folkenberg, and A. Bjarklev, J. Lightwave Technol. **22**, 11 (2004).
20. T. A. Birks, F. Luan, G. J. Pearce, A. Wang, J. C. Knight, and D. M. Bird, Opt. Express **14**, 5688 (2006).
21. P. J. Roberts, F. Couny, H. Sabert, B. J. Mangan, D. P. Williams, L. Farr, M. W. Mason, A. Tomlinson, T. A. Birks, J. C. Knight, and P. S. J. Russell, Opt. Express **13**, 236 (2005).
22. N. K. Baddela, M. N. Petrovich, Y. Jung, J. R. Hayes, N. V. Wheeler, D. R. Gray, N. Wong, F. Parmigiani, E. Numkam, J. P. Wooler, F. Poletti, and D. J. Richardson, in *CLEO/QELS* (2013), paper CTu2K.3.
23. A. M. Jones, A. V. V. Nampoothiri, A. Ratanavis, T. Fiedler, N. V. Wheeler, F. Couny, R. Kadel, F. Benabid, B. R. Washburn, K. L. Corwin, and W. Rudolph, Opt. Express **19**, 2309 (2011).